CrystEngComm

Accepted Manuscript

ROYAL SOCIETY OF CHEMISTRY

www.rsc.org/crystengcomm

CrystEngComm

ARTICLE

Halogen bonding in multi-connected 1,2,2-triiodo-alkene involving geminal and/or vicinal iodines: A crystallographic and DFT study

Received 00th January 20xx,
Accepted 00th January 20xx

DOI: 10.1039/x0xx00000x

www.rsc.org/

G. Berger,[a,b] K. Robeyns,[c] J. Soubhye,[a] R. Wintjens,[d] and F. Meyer[d*]

Four halogen bonded arrangements of (1,2,2-Triiodovinyl)benzene involving geminal and/or vicinal iodine atoms were studied both by X-ray diffraction and density functional theory (DFT). Crystallographic data show weaker XB-type interactions for the iodine atom geminal to the phenyl, which is corroborated by the DFT-optimized structures of 1:1, 1:2 and 1:3 (1,2,2-triiodovinyl)benzene/pyridine complexes. In addition, the theoretical model reflects the interplay existing between these conjugated and multi-connected sites, highlightning the weakening of the halogen bonds when the number of partners are increased.

Introduction

Over the last 30 years, supramolecular chemistry has arisen as a major player in the design of highly functional materials.[1] The creation of ever more sophisticated building blocks combined to a prominent source of interactions allowed for an increase in complexity through self-organization.[2] Recently, the field of halogen bonding (XB) has emerged as a rational and reliable strategy to design supramolecular complexes with varied topological structures.[3,4,5] A step forward, appealing applications of this intriguing non-covalent bond were extended to the formation of functional materials.[6,7] Hence, purposely-built systems have been applied as supramolecular liquid crystals,[8,9] phosphorescent and photo-responsive materials,[10,11] ion sensors,[12] dendrimers,[13] catalytic systems[14,15] and gels.[16] As far as biological properties are concerned, a survey of the protein data bank emphasized several halogen bonded complexes,[17,18] including the main thyroid hormone,[19] and constant efforts are made in drug discovery using theoretical methods.[20]

Considering the anisotropic charge distribution around the halogen nuclei, the main feature of these atoms lies in a positive area (the so-called σ-hole) located along the extension of a C-X bond and resulting from the depletion of the outer lobe of the C-X bonding orbital.[21,22] This positive region that is responsible for the halogen bonds renders them highly directional,[23,24] the remaining atom surface being covered by a negative electrostatic potential. The extent of the σ-hole is related to the XB interaction strength and normally follows the trend I > Br > Cl. However, neighbouring electron withdrawing groups can also increase this area, accounting for a strengthening of the XB interaction.[25]

It has recently been demonstrated that a synergistic effect can take place in certain supramolecular systems possessing concomitant interactions, giving rise to a competitive or cooperative phenomenon. Accurate modulation of interaction strengths can therefore happen by careful structural design, these aspects being mainly reported by theoretical studies through association of XB with anion-π,[26] cation-π,[27] π-π[28,29] or lone-pair-π[30] interactions. In this regard, a triiodoalkene derivative composed of three conjugated XB donor sites provides an appealing model to understand both the interplay between several interacting groups and the variation of the electrostatic potential covering these halogens. Indeed, a comparison of multiply-connected synthons involving vicinal (*cis* or *trans* position) or geminal iodine atoms have never been reported so far. Considering the dual character of halogens serving both as electron donors and acceptors, a slight variation in the electron density of the halogen can drastically affect a supramolecular organization. We herein studied the X-ray structure of (1,2,2-triiodovinyl)benzene which is composed of 4 different arrangements involving geminal and vicinal XB sites. The supramolecular organization is governed by two types of I···I and I···π halogen bonds where iodine atoms behave as XB donors and acceptors. In order to shed light on the crystallographic parameters, we proceeded with density

---

[a] *Chimie Pharmaceutique Organique, Faculty of pharmacy, Université Libre de Bruxelles (ULB), Boulevard du Triomphe, 1050 Bruxelles, Belgium*
[b] *Department of Chemistry, Massachusetts Institute of Technology, Cambridge, MA 02139, United States*
[c] *Institute of Condensed Matter and Nanosciences (IMCN), Université Catholique de Louvain (UCL), Bâtiment Lavoisier - Place Louis Pasteur 1, 1348 Louvain-la-Neuve, Belgium.*
[d] *Laboratory of biopolymers and supramolecular nanomaterials, Faculty of pharmacy, Université Libre de Bruxelles (ULB), Boulevard du Triomphe, 1050 Bruxelles, Belgium*
Correspondence e-mail: franck.meyer@ulb.ac.be

† Footnotes relating to the title and/or authors should appear here.

---

[e] *Electronic Supplementary Information (ESI) available: [Synthetic procedure, X-ray crystallography, Crystal data and structure refinement details, DFT calculation). See DOI: 10.1039/x0xx00000x*

functional theory (DFT) models of halogen bonded complexes comprised of (1,2,2-triiodovinyl)benzene in the presence of one, two and three pyridine partners.

Preparation of triiodoalkene

(1,2,2-Triiodovinyl)benzene was unexpectedly formed during the synthesis of (iodoethynyl)benzene. Iodoalkynes are frequently used as XB synthons,[31,32,33] and represent a good entry to 5-iodo-1,2,3-triazoles through copper-catalyzed azide–alkyne cycloaddition reaction.[34] When iodination of phenylacetylene was carried out with potassium hydroxide and iodine at room temperature for 20 h, the expected iodoalkyne was accompanied by a few percent of (1,2,2-triiodovinyl)benzene. However, this triiodoalkene was obtained in 85% yield by reaction of (iodoethynyl)benzene with an excess of iodine in dioxane. The resulting compound crystallized as a colourless material after a period of several weeks at 4 °C. A literature survey revealed that the synthesis of this compound has been scarcely reported over the last 40 years, yet NMR data and melting point (110 °C) confirmed the structure.[35,36,37] A step further, synthons possessing a triiodoethenyl group are not so common. Focusing on the X-ray structures of such molecules, the Cambridge Structural Database revealed that only three supramolecular complexes were deposited. In 2002, the 1:1 co-crystal of 1,1,2,3,4,4-hexaiodobuta-1,3-diene and 1,7-phenanthroline was supported by N···I halogen bonds; the authors were unable to obtain the hexaiodobuta-1,3-diene in pure form. Subsequently, Bouchmella and co-workers reported the structure of 1-(2,3,3-triiodoallyl)imidazole which was comprised of N···I contacts. In addition, this triiodoimidazole was allowed to arrange into a halogen bonded supramolecular complex with morpholinium iodide due to I···I$^-$ interactions.[38]

X-ray structure analysis of halogen bonded compound

In our case, the crystallization of (1,2,2-triiodovinyl)benzene allowed the determination of its X-ray structure through analysis of one single crystal. Two molecules are present in the asymmetric units, both showing disorder. After refinement, the crystal structure of (1,2,2-triiodovinyl)benzene consists in the combination of four different organizations. The compound crystallized in the non-centrosymmetric space group Cc, with 8 molecules packed in the unit cell.

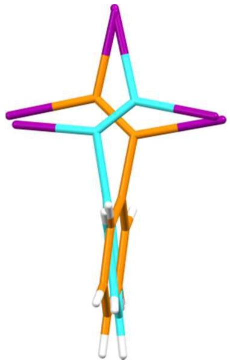

Figure 1: Stick representation showing the observed disorder, the nature of the disorder conserves the position of the I-atoms, the carbon atoms of both parts are coloured in cyan and orange (the disorder observed for the second molecule is of similar nature).

Results and discussion

The observed disorder is similar in both molecules and consists of a 180° rotation around the principal axis of the molecule (Figure 1), while preserving the positions of the I-atoms, making the disorder largely restricted to the orientation of the central double bond. The occupancy of the disordered parts of both molecules were refined and where the occupancies for the first molecule (C1>I11) are evenly distributed over both parts (49/51), the second molecule (C21>I31) shows an unbalanced ratio of 66/34. The measured crystal was non-merohedrally twinned over 3 domains (2 fold rotation around the reciprocal [4 4 -1] and the direct [1 1 0] axes, with small twin fractions about 9% each).

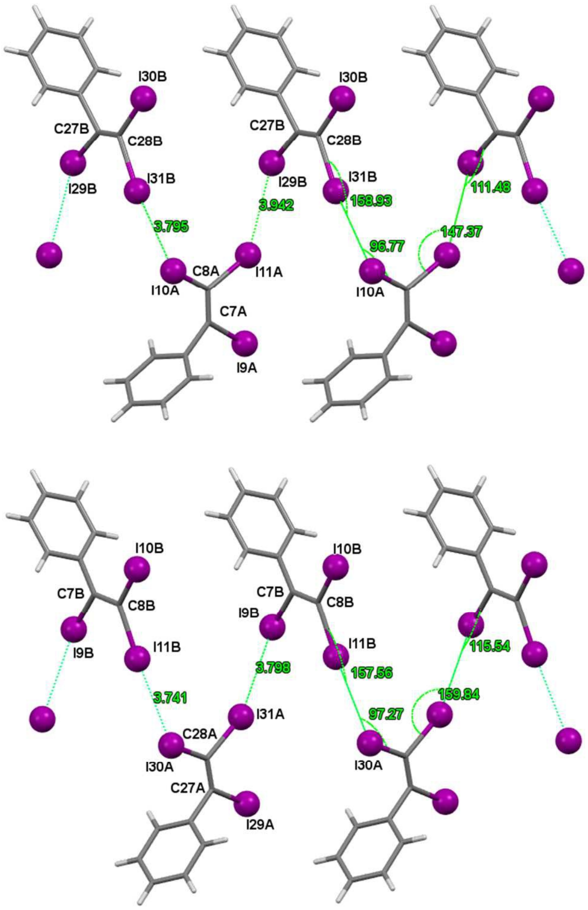

Figure 2. X-ray structures of forms **1** (top) and **4** (bottom) highlighting the features of I···I halogen bonds. For the sake of clarity, carbon (grey) and hydrogen (white) atoms are represented in capped sticks, and iodine (purple) atoms are in ball and stick.

By combination of both disordered parts of both molecules, 4 (2x2) different arrangements can be described. Form **1**: C1A to I11A and C21B to I31B; form **2**: C1A to I11A and C21A to I31A;

form **3**: C1B to I11B and C21B to I31B; form **4**: C1B to I11B and C21A to I31A. The measured crystal can be seen as consisting of 4 subdomains (forms **1**-**4**), of which form **3** is most abundantly present.

From the topological point of view, the units develop a wavy polymeric organization[39,40] involving I···I contacts supported by other I···π interactions.[41] In addition, the phenyl ring is twisted out of the tri-iodoalkene plane, almost perpendicular in all cases (79.07-89.47°). By focusing on the interacting iodine atoms, the four forms **1-4** lie in different modes of connections. Infinite chains in forms **1** and **4** consist of units involving in one case geminal iodine atoms (I-C-I angle around 120°), and in the other vicinal atoms in *cis* position (I-C-I angle < 90°). In contrast, forms **2** and **3** demonstrate a symmetrical arrangement since both modules are bound thanks to geminal iodine atoms in **2** and vicinal atoms in **3**.

Regarding halogen···halogen interaction geometries, the literature refers to them as type I and type II.[42,43,44] In substance, an arrangement of type I occurs when $\Theta_1 \approx \Theta_2$ (where Θ_1 and Θ_2 are the $R\text{-}X_1\cdots X_2$ and $X_1\cdots X_2\text{-}R$ angles, respectively), and the second possibility arises in perpendicular arrangements, namely $\Theta_1 \approx 180°$ and $\Theta_2 \approx 90°$ (halogen bonding).

Forms **1** and **4** are featured with a type II interaction (Figure 2). In form **1**, the inter-halogen distances between I10A···I31B and I11A···I29B are 3.795 and 3.942 Å, respectively, which is slightly shorter than the sum of their van der Waals radii (3.96 Å).[45] The I10A···I31B interaction is clearly identified as a halogen bond due to the C28B-I31B···I10A and C8A-I10A···I31B angles of 158.9° and 96.8°, respectively. In addition, the longer inter-iodine atom distance (3.942 Å) is associated with C8A-I11A···I29B and C27B-I29B···I11A angles of 147.4° and 111.5°, respectively, which tends to be ascribed to a very weak type II interaction (Figure 2). Finally, the supramolecular scaffold is also stabilized by supplementary H···I hydrogen bonds (the sum of their van der Waals radii being 3.18 Å).[46,47] For instance, the I9A···H2A interaction (distances = 2.992 Å) connects successive units of the same infinite chains while parallel wavy organizations are linked via I31B···H1A contacts (distances = 2.942 Å). The less directional character of the hydrogen bonds compared to XB is given by the values of C2A-I9A···H2A and C1A-I31B···H1A angles which are 149.4° and 127.6°, respectively. In contrast, the electron donation from the negative equatorial region of iodine atoms is highlighted by the I9A···H2A-C7A and I31B···H1A-C28B angles close to 90° (109.5° and 87.5°, respectively).

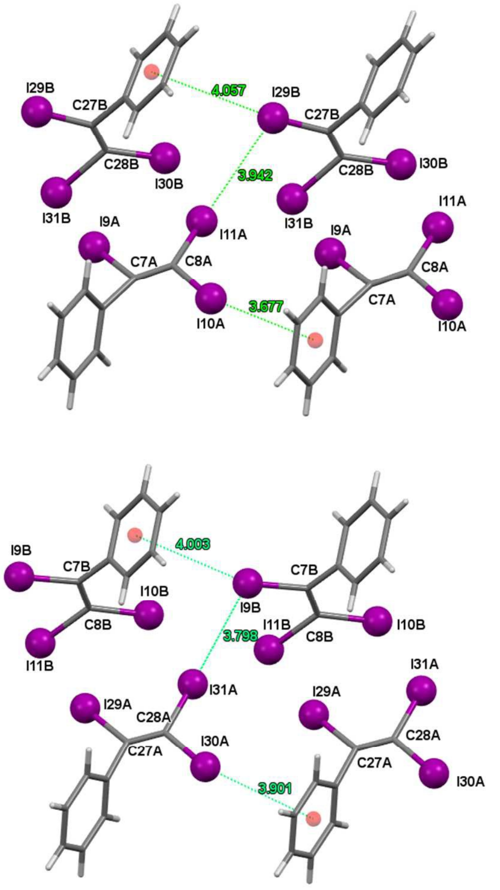

Figure 3. X-ray structures of forms **1** (top) and **4** (bottom) showing the I···Ar halogen bonds.

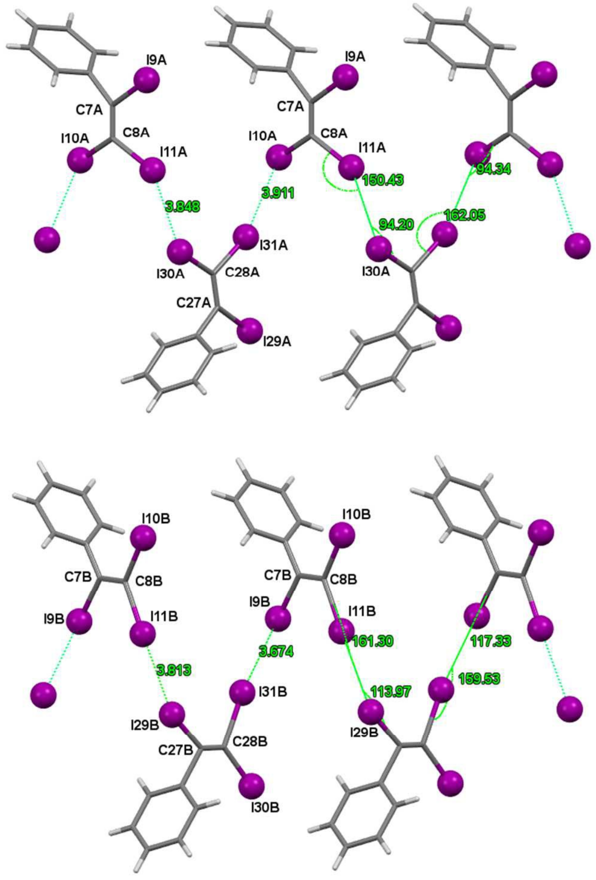

Figure 4. X-ray structures of forms **2** (top) and **3** (bottom) highlighting the features of I···I halogen bondings.

Parameters of the intermolecular contacts displayed by form **4** mirrored those found in form **1**. I···I distances are in the range 3.74-3.80 Å, consistent with XB contacts. The C8B-I11B···I30A and C28B-I30A···I11B angles are almost similar to those observed in form **1** (157.6° and 97.3°, respectively), which is in agreement with an electron donation from I30A toward I11B (d = 3.741 Å). As concerns I31A and I9B, the C28A-I31A···I9B angle of **4** (115.5°) is almost similar to the C27B-I29B···I11A angle of form **1** and is consequently an interaction of type II (halogen bonding). In contrast, the C7B-I9B···I31A angle of **4** appears more open than the C8A-I11A···I29B angle of **1** with a value of 159.8° (Figure 2). The main difference lies in the absence of hydrogen bonds in form **4** with respect to **1**. Indeed, in form **4** the distance between I29A and H25A or H24A are 3.951 Å and 3.781 Å, respectively, which is much longer than the I9A···H2A separation found in **1**. In the same way, I11B and H25A are separated by a distance of 3.316 Å, which is 10% longer than the I31B···H1A interactions in **1**. I10A and I29B of form **1** are also involved in halogen bonds with neighbouring aromatic rings. The same behaviour is observed for I9B and I30A of form **4**.

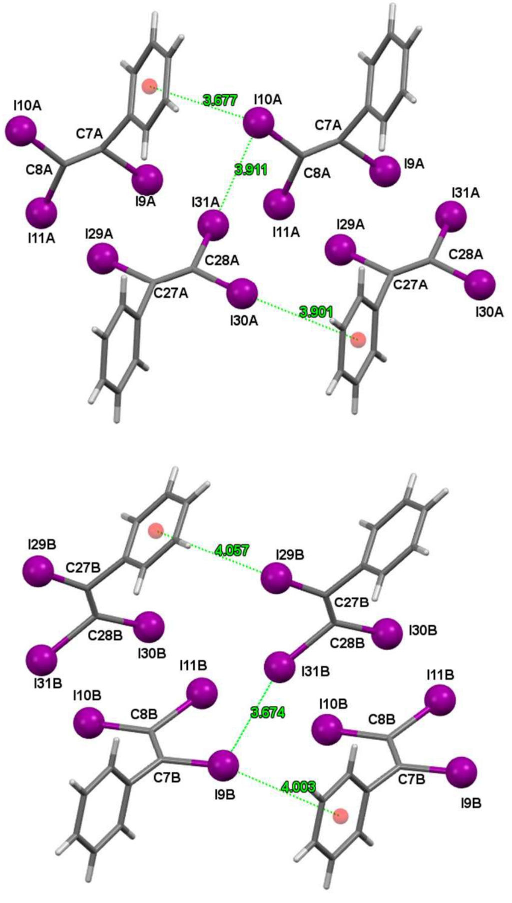

Figure 5. X-ray structures of forms **2** (top) and **3** (bottom) showing the I···Ar halogen bonds.

Measurement of the halogen···phenyl centroid (Ce) separations in system **1** gives the following values: I10A···Ce distance = 3.677 Å and I29B···Ce distance = 4.057 Å. The typical angular parameters of XB species were thereby determined, i.e. C8A-I10A···Ce and C2A-Ce···I10A angles of 151.16° and 76.69°, respectively, and C27B-I29B···Ce and C24B-Ce···I29B angles of 151.57° and 67.17°, respectively (reported values used the smallest Car-Ce···I angles). In **4**, I···Ph (centroid) distances are almost the same, i.e. 4.003 Å and 3.901 Å for I9B···Ce and I30A···Ce contacts, respectively (Figure 3). Regarding the angles, the values for C28A-I30A···Ce and C7B-I9B···Ce angles are close to 150° (143.30° and 155.89°, respectively) whereas the C24A-Ce···I30A and C2B-Ce···I9B angles correspond to almost 60° which is in line with XB parameters (64.43° and 63.52°, respectively).

When geminal (form **2**) or vicinal (form **3**) atoms of both molecules are bound by inter-halogen interactions, the halogen···halogen crystallographic parameters appear slightly different (Figure 4).

For instance, the halogen bonded I11A···I30A atoms of system **2** feature a distance of 3.848 Å, and C8A-I11A···I30A and C28A-I30A···I11A angles of 150.4° and 94.2°, respectively. The same trend is observed for the other I10A···I31A interaction, since iodine atoms are separated by a distance of 3.911 Å, and the C8A-I10A···I31A and C28A-I31A···I10A angles are 94.3° and 162.1°, respectively. As for system **1**, successive units of **2** are bound thanks to I9A···H2A hydrogen bonds (distances = 2.992 Å) and parallel zig zag arrangements are linked via I31A···H1A contacts (distances = 3.038 Å). Other structural parameters also arise similar to that found in **1**. Hence, the C2A-I9A···H2A and C28A-I31A···H1A angles tend to be linear (149.4° and 130.1°, respectively), whereas I9A···H2A-C7A and I31A···H1A-C1A angles are almost perpendicular (109.5 and 107.6°, respectively). I···I distances in form **3** are nearly the same, although the I31B···I9B contact appears the shortest (3.674 Å) among all inter-halogen interactions. However, the C-I···I angles associated with these non-covalent bonds are different from the previous case. Indeed, two values are close to 115° whereas the other ones are around 160° (Figure 4). In both cases, the arrangement remains governed by type II halogen···halogen interactions. This organization is also characterized by the absence of hydrogen bonds since the closest distances I10B···H2B and I31B···H1B are larger than 3.41 Å.

Table 1. C-I···Ce and Ce-Car···I angles found for complexes **2** and **3.**

X-ray structures	C-I···Ce angles	Ce-Car···I angles
Form **2**	151.5° (C8A-I10A···Ce) 143.3° (C28A-I30A···Ce)	76.7° (C2A-Ce···I10A) 64.4° (C24A-Ce···I30A)
Form **3**	151.6° (C27B-I29B···Ce) 159.9° (C7B-I9B···Ce)	67.2° (C24B-Ce···I29B) 63.5° (C2B-Ce···I9B)

Forms **2** and **3** are also supported by I···Ph halogen bonds (Figure 5). Interestingly, when molecules of form **2** are bound by means of geminal iodine atoms, I···Ce (centroid) distances are particularly short (3.677 Å and 3.901 Å). In contrary, the organization governed by vicinal halogen atoms (form **3**) endows longer I···Ce (centroid) contacts up to 4.057 Å. The angular parameters featuring these interactions are reported in Table 1 and follow the trend observed for complexes **1** and **4**.

At this stage, the crystallographic parameters afford to distinguish different levels of interaction depending on the involved iodine.

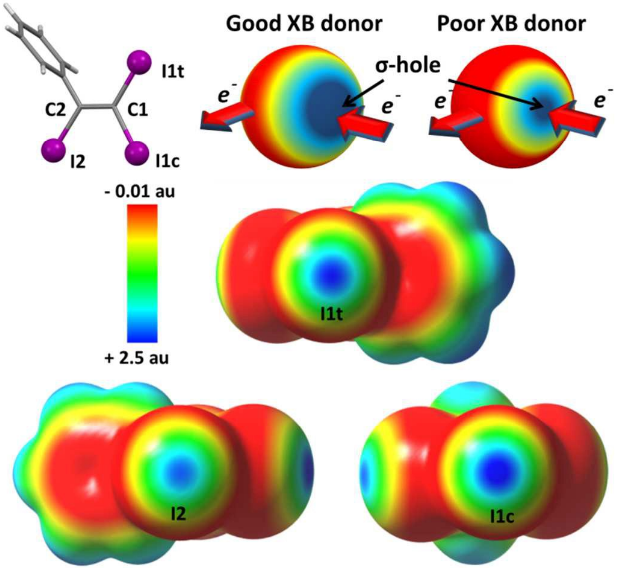

Figure 6. (1,2,2-triiodovinyl)benzene with labelled carbon and iodine atoms (up left). Schematic views of halogen atoms (up right) highlighting the anisotropic charge distribution for good and poor XB donors. The σ-hole (positive region in blue) and negative annulus (red region) cover varied area. Electrostatic potential map for I1t, I2 and I1c at the ωB97X-D/def2-TZVP level (bottom; density isovalue = 0.0004 au) (down).

For the sake of clarity and a comparison of the different forms, we propose to relabel the atoms as follows: carbon C1 is linked to two iodine atoms I1c (*cis* position relative to I2) and I1t (*trans* position relative to I2) and carbon C2 is linked to iodine I2 and phenyl group (Figure 6). Taking into consideration the supramolecular organizations **1** to **4**, it can be observed that short I···Ce distances (d ≤ 3.901 Å) involving I1t atoms are present in forms **1**, **2** and **4**. In addition, the same halogen (I1t) behaves as an electron donor toward an iodine atom (I1c), giving rise to C-I1t···I1c angles of about 95°. In contrast, longer I···Ce contacts (d ≥ 4.003 Å) are noticed when the chains involve I2 halogens (forms **1**, **3** and **4**), resulting in similar C-I2···I1c angles (~ 115°) (Figure 3 and Figure 5).

DFT study

These aspects have convinced us to study this phenomenon using DFT and model complexes. Purposely, we decided to model varied supramolecular complexes involving (1,2,2-triiodovinyl)benzene in the presence of one, two or three pyridine partners as electron donors. Pyridine was chosen owing to the fact that many supramolecular XB scaffolds are endowed with a pyridyl functionality. In addition, this molecule is frequently used as model system for theoretical and analytical investigations targeting the particular features of halogen bonding.[48,49]

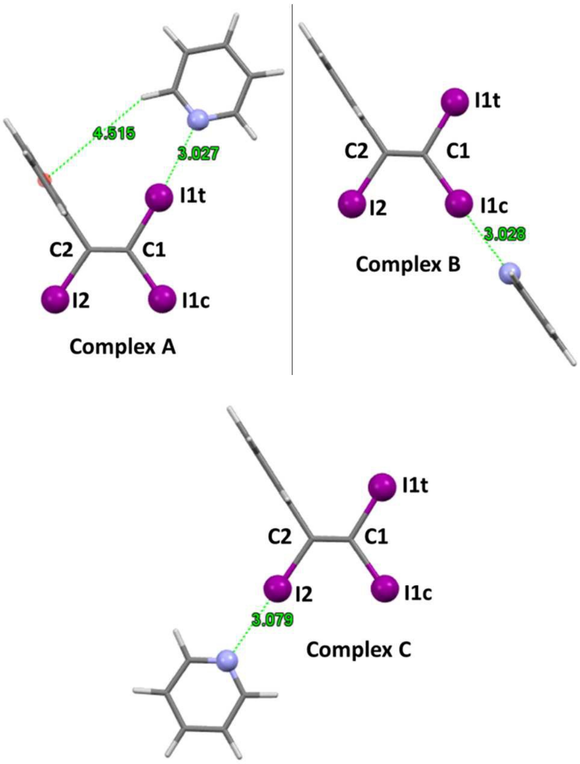

Figure 7. DFT-optimized structures of halogen bonded complexes **A** (top left), **B** (top right) and **C** (bottom) composed of 1,2,2-triiodovinyl)benzene and pyridine in a 1:1 ratio.

All the complexes were fully optimized using the ωB97X-D exchange correlation functional[50] together with the def2-TZVP basis set from Ahlirchs and co-workers,[51,52] except iodine for which the quasi-relativistic Stuttgart/Dresden pseudo-potential was used. Whereas conventional exchange-correlation functionals lack an accurate description of London dispersion forces,[53,54] the ωB97X-D functional includes DFT-D semi-classical correction and performs particularly well against *ab initio* methods.[55,56] Optimized geometries were verified by frequency calculations as minima (i.e. zero imaginary frequencies) and free energies were corrected to account for the zero-point energy.

First, the electrostatic potential map for (1,2,2-triiodovinyl)benzene at the ωB97X-D/def2-TZVP level highlights a slightly larger σ-hole for I1t by comparison with I2. This observation echoes the more open C-I2···I1c angles with respect to C-I1t···I1c angles of X-ray structures **1-4** (Figure 6).

Then, three supramolecular complexes **A**, **B** and **C** composed of (1,2,2-triiodovinyl)benzene and pyridine involving one iodine atom were studied. This series gives some information regarding the XB donor properties of each site. N···I1c and N···I1t distances from complexes **A** and **B** are nearly the same, namely a separation of about 3.03 Å. Complex **A** features a perpendicular organization of the pyridine and the phenyl ring, with a short H···Ph (centroid) distance of 4.515 Å (Figure 7), but this interaction should only weakly interfere with the XB counterpart. The N···I2 halogen bond is found weaker in complex **C** with respect to **A** and **B**, as determined by a longer N···I distance of 3.08 Å (Figure 7). These samples highlight I1c and I1t as better XB donor with respect to I2.

The same trend is observed by comparison with the X-ray structures of forms **1** to **4**. Both molecules in the asymmetric unit are involved in I···Ph contacts, one through I2 (geminal to Ph), the other through I1t (cis position relative to Ph). I2 atoms of forms **1**, **3** and **4** however make weaker halogen bonds (distance > 4.003 Å) than Ph···I1t interactions (distance < 3.901 Å) found in forms **1**, **2** and **4** (Table 2).

Table 2. I···Ce distances involving I2 (geminal to Ph) and I1t (cis position relative to Ph) determined for complexes **1** to **4**

X-ray structures	I1t···Ce distances	I2···Ce distances
Form **1**	3.677 Å (I10A)	4.057 Å (I29B)
Form **2**	3.901 Å (I30A) 3.677 Å (I10A)	-
Form **3**	-	4.057 Å (I29B) 4.003 Å (I9B)
Form **4**	3.901 Å (I30A)	4.003 Å (I9B)

These DFT models thus corroborate the decreasing order of binding strength of iodine atoms I1c ≈ I1t > I2, following the observations made in crystalline forms **1** to **4**.

In a second step, theoretical supramolecular systems involving 2 iodine atoms were studied (complexes **D**, **E** and **F**). These complexes better mimic the I···I and I···Ph contacts found in X-ray structures **1** to **4**. These calculations were run to emphasize any synergistic effect (competition or cooperation) when two conjugated sites are involved in a XB interaction. Complex **D** is particularly interesting in terms of supramolecular organization and structural parameters. Both N···I2 and N···I1t interactions appear weaker than in the dimeric systems owing to a lengthening of 1.3 and 2% with respect to complexes **C** and **A**, respectively (N···I2 distance = 3.12 Å and N···I1t distance = 3.09 Å). Whereas the pyridine unit bound to I2 is twisted in an orthogonal fashion with regard to the pyridine moiety of complex **C**, the other module maintains the same relative arrangement featuring a very weak H···Ph hydrogen bond 10% shorter than in structure **A**. It is worthy to note that such a hydrogen bond should not deeply affect the strength of the neighbouring halogen bond. This assumption seems reasonable since the N···I distances are close under similar conditions, whether or not this H···Ph is observed on the optimized complex (complexes **D** and **E**). The simultaneous electron donation from the pyridine units to I1t and I2 provokes an increase of electronic density for both XB donor sites, which thereby become less favorable electron acceptors. Complex **E** also possesses a double N···I1t and N···I1c interaction, similar to that observed in the X-ray forms **1**, **2** and **4**. In this case, the pyridine unit bound to I1t is perpendicular to the triiodo core, and consequently, no hydrogen bond (H···Ph) is observed.

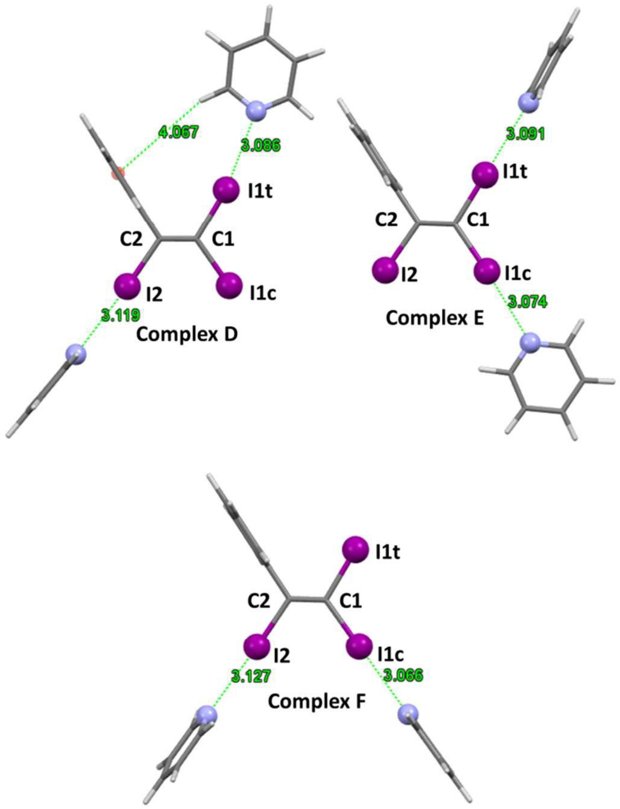

Figure 8. DFT-optimized structures of halogen bonded complexes **D** (top left), **E** (top right) and **F** (bottom) composed of 1,2,2-triiodovinyl)benzene and pyridine in a 1:2 ratio.

However, the variation of intermolecular distances follows the same trend as seen with complex **D**, namely a slight increase of N···I1t (3.09 Å) and N···I1c (3.07 Å) separations of 2.1 and 1.5%, respectively, with regard to complexes **A** and **B**. Again the double electron donating contribution tends to decrease the propensity of both iodine atoms to accept electrons from their partner, but I1c seems to be less affected. Finally, complex **F** shows the same increase of interatomic distance compared to systems **B** and **C**, namely N···I1c and N···I2 contacts of 3.07 and 3.13 Å, respectively, which represents a lengthening of 1.3 and 1.5%, respectively. From the general point of view, the N···I2 halogen bonds remain by far the weakest interaction in all theoretical supramolecular architectures **D**, **E** and **F** following the same trend observed in crystalline forms **1** to **4**: N···I2 distances > 4.00 Å and N···I1t or N···I1c distances < 3.94 Å. As far as simultaneous N···I1t and N···I1c contacts are concerned, X-ray structures **1**, **2** and **4** differ from modelling results since only one unit of structure **4** follows this trend. At this stage, we can admit the limitation of our computational models since crystal architectures are governed by two types of I···I and I···π halogen bonds in addition to a dual nature of iodine atoms which behave both as XB donors and acceptors.

At last, we evaluated the four-membered complex **G** comprised of (1,2,2-triiodovinyl)benzene and three pyridine partners (Figure 9). As expected, concomitant N···I halogen bonds produce an overall weakening of these interactions. N···I2, N···I1t and N···I1c distances are calculated at 3.18, 3.13 and 3.11 Å, respectively, which correspond to an increase around 3% by comparison with values found in complexes **C**, **A** and **B**. Though, we can note a more pronounced lengthening for N···I2 interaction which is probably due to the combined role of the two C1-I···N halogen bonds.

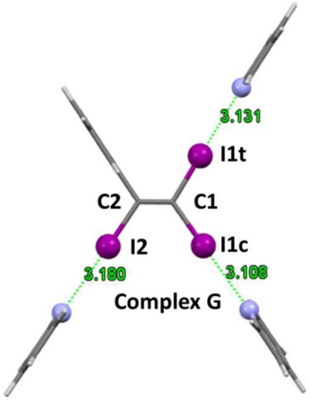

Figure 9. DFT-optimized structures of halogen bonded complexes **F** composed of 1,2,2-triiodovinyl)benzene and pyridine in a 1:3 ratio.

Conclusions

One of the very first supramolecular arrangements of a triiodoalkene derivative was studied by means of X-ray crystallography and DFT. The crystal structure of 1,2,2-triiodovinyl)benzene lies in the combination of four different organizations governed by two types of I···I and I···π halogen bonds involving vicinal or geminal iodine atoms. Crystallographic parameters highlight weaker interactions when an iodine atom (I2) geminal to the phenyl ring behaves as a XB donor by comparison with I1t (in *trans* position relative to I2). DFT-optimized structures of 1:1, 1:2 and 1:3 (1,2,2-triiodovinyl)benzene/pyridine complexes correlate well and show longer N···I2 distances compared to N···I1t contacts. However, computational models differ from the X-ray structures regarding the halogen bonds involving geminal iodine atoms. This aspect is probably assigned to the dual electron donor/acceptor character of I1t in the crystalline forms but absent in our computational models. However, a comparison of the theoretical systems reflects the interplay existing between conjugated and multi-connected sites. The N···I halogen bonds appear weaker in going from 1:1 to 1:2 to 1:3 (1,2,2-triiodovinyl)benzene/pyridine complexes, consistent with an electron density increase on the conjugated iodine atoms, in response to the formation of the first halogen bonds and thus decreasing their propensity to accept electrons from another partner. The careful design of iodinated alkenes can propose an original strategy to construct complicated supramolecular architectures, considering the dual XB donor/acceptor role of these atoms. In addition, these triiodoalkene derivatives have recently found some application in materials science for their fungicide and antibacterial properties.

Acknowledgements

G. Berger thanks the ULB-VUB computing centre for providing high performance computing facilities and useful technical support.

Notes and references

‡ Footnotes relating to the main text should appear here. These might include comments relevant to but not central to the matter under discussion, limited experimental and spectral data, and crystallographic data.

---

1 P. A. Gale and J. W. Steed. *Supramolecular Chemistry: from molecules to nanomaterials*. 1st ed. New York: John Wiley & Sons Ltd; 2012.
2 J. M. Lehn, *Proc. Natl. Acad. Sci. USA* 2002, **99**, 4763-4768.
3 P. Metrangolo, F. Meyer, T. Pilati, G. Resnati and G. Terraneo, *Angew. Chem. Int. Ed. Engl.*, 2008, **47**, 6114–6127.
4 K. Rissanen, *CrystEngComm*, 2008, **10**, 1107-1113.
5 L. C. Gilday, S. W. Robinson, T. A. Barendt, M. J. Langton, B. R. Mullaney and P. D. Beer, *Chem. Rev.*, 2015, **115**, 7118–7195.
6 F. Meyer and P. Dubois, *CrystEngComm*, 2013, **15**, 3058–3071.
7 A. Priimagi, G. Cavallo, P. Metrangolo and G. Resnati, *Acc. Chem. Res.*, 2013, **46**, 2686–2695.
8 H. L. Nguyen, P. N. Horton, M. B. Hursthouse, A. C. Legon and D. W. Bruce, *J. Am. Chem. Soc.* 2004, **126**, 16-17.
9 D. W. Bruce, P. Metrangolo, F. Meyer, T. Pilati, C. Präsang, G. Resnati, G. Terraneo, S. G. Wainwright and A. C. Whitwood, *Chem. Eur. J.* 2010, **16**, 9511-9524.
10 O. Bolton, K. Lee, H.-J. Kim, K. Y. Lin and J. Kim, *Nat. Chem.* 2011, **3**, 205-210.
11 A. Priimagi, M. Saccone, G. Cavallo, A. Shishido, T. Pilati, P. Metrangolo and G. Resnati, *Adv. Mater.* 2012, **24**, OP345-352.
12 A. Caballero, F. Zapata, N. G. White, P. J. Costa, V. Félix and P. D. Beer, *Angew. Chem. Int. Ed.*, 2012, **51**, 1876-1880.
13 P. Metrangolo, F. Meyer, T. Pilati, D. M. Proserpio and G. Resnati, *Cryst. Growth Des.*, 2008, **8**, 654–659.
14 A. Bruckmann M. Pena and C. Bolm, *Synlett* 2008, 900-902.
15 O. Coulembier, F. Meyer and P. Dubois, *Polym. Chem.* 2010, **1**, 434-437.
16 L. Meazza, J. A. Foster, K. Fucke, P. Metrangolo, G. Resnati and J. W. Steed, *Nat. Chem.* 2013, **5**, 42-47.
17 P. Auffinger, F. A. Hays, E. Westhof and P. S. Ho, *Proc. Natl. Acad. Sci. U.S.A.*, 2004, **101**, 16789-16794.
18 R. Wilcken, M. O. Zimmermann, A. Lange, A. C. Joerger and F. M. Boeckler, *J. Med. Chem.*, 2013, **56**, 1363-1388.
19 S. Mondal and G. Mugesh, *Angew. Chemie Int. Ed.*, 2015, **54**, 10833–10837.
20 Z. Xu, Z. Yang, Y. Liu, Y. Lu, K. Chen and W. Zhu, *J. Chem. Inf. Model.*, 2014, **54**, 69–78.
21 T. Clark, M. Hennemann, J. S. Murray and P. Politzer, *J. Mol. Model.* 2007, **13**, 291-296.

22 L. P. Wolters, P. Schyman, M. J. Pavan, W. L. Jorgensen, F. M. Bickelhaupt and S. Kozuch, *WIREs Comput. Mol. Sci.* 2014, **4**, 523-540.
23 L. Brammer, E. A. Bruton and P. Sherwood, *Cryst. Growth Des.* 2001, **1**, 277-290.
24 C. B. Aakeröy, M. Fasulo, N. Schultheiss, J. Desper and C. Moore, *J. Am. Chem. Soc.* 2007, **129**, 13772-13773.
25 K. E. Riley, J. S. Murray, J. Fanfrlík, J. Rezáč, R. J. Solá, M. C. Concha, F. M. Ramos and P. Politzer, *J. Mol. Model.* 2011, **17**, 3309-3318.
26 C. Estarellas, A. Frontera, D. Quiñonero and P. M. Deyà, *ChemPhysChem*, 2011, **12**, 2742–2750.
27 Y. Lu, Y. Liu, H. Li, X. Zhu, H. Liu and W. Zhu, *ChemPhysChem*, 2012, **13**, 2154–2161.
28 H. Li, Y. Lu, Y. Liu, X. Zhu, H. Liu and W. Zhu, *Phys. Chem. Chem. Phys.*, 2012, **14**, 9948-9955.
29 S. V. Rosokha and E. a. Loboda, *J. Phys. Chem. A*, 2015, **119**, 3833–3842.
30 G. Berger, J. Soubhye, A. van der Lee, C. Vande Velde, R. Wintjens, P. Dubois, S. Clément and F. Meyer, *Chempluschem*, 2014, **79**, 552–558.
31 O. Dumele, D. Wu, N. Trapp, N. Goroff and F. Diederich, *Org. Lett.*, 2014, **16**, 4722–4725.
32 M. Saccone, V. Dichiarante, A. Forni, A. Goulet-Hanssens, G. Cavallo, J. Vapaavuori, G. Terraneo, C. J. Barrett, G. Resnati, P. Metrangolo and A. Priimagi, *J. Mater. Chem. C*, 2015, **3**, 759–768.
33 C. B. Aakeröy, M. Baldrighi, J. Desper, P. Metrangolo and G. Resnati, *Chem. Eur. J.*, 2013, **19**, 16240–16247.
34 J. E. Hein, J. C. Tripp, L. B. Krasnova, K. B. Sharpless and V. V. Fokin, *Angew. Chem. Int. Ed.*, 2009, **48**, 8018–8021.
35 M. J. Cohen and E. McNelis, *J. Org. Chem.*, 1984, **5**, 515–518.
36 A. Pelter and R. A. Drake, *Tetrahedron Lett.*, 1988, **29**, 4181–4184.
37 M. J. Dabdoub, J. V. Comasseto, S. M. Barros and F. Moussa, *Synth. Commun*., 1990, **20**, 2181-2183.
38 K. Bouchmella, B. Boury, S. G. Dutremez and A. Van Der Lee, *Chem. Eur. J.*, 2007, **13**, 6130–6138.
39 A. De Santis, A. Forni, R. Liantonio, P. Metrangolo, T. Pilati and G. Resnati, *Chem. Eur. J.*, 2003, **9**, 3974-3983.
40 P. Metrangolo, F.Meyer, T. Pilati, G. Resnati and G. Terraneo, *Acta Cryst.,* 2007, E**63**, o4243.
41 G. Berger, J. Soubhye and F. Meyer, *Polym. Chem.*, 2015, **6**, 3559–3580.
42 F. F. Awwadi, R. D. Willett, K. A. Peterson and B. Twamley, *Chem. Eur. J.*, 2006, **12**, 8952–8960.
43 L. Brammer, G. Mínguez Espallargas and S. Libri, *CrystEngComm*, 2008, **10**, 1712-1727.
44 D. J. R. Duarte, N. M. Peruchena and I. Alkorta, *J. Phys. Chem. A*, 2015, **119**, 3746–3752.
45 A. Bondi, *J. Phys. Chem*. 1964, **68**, 441–451.
46 R. Bishop *CrystEngComm* 2015, **17**, 7448-7460.
47 G. R. Desiraju *Chem. Comm*. 2005, **24**, 2995-3001.
48 Q. Shi, H. Su, Y. Liu, W. Wu and Y. Lu, *Comput. Theor. Chem.*, 2014, **1027**, 79–83.
49 B. Hawthorne, H. Fan-Hagenstein, E. Wood, J. Smith and T. Hanks, *Int. J. Spectrosc.*, 2013, **2013**, Article ID 216518.
50 J.-D. Chaia, and M. Head-Gordon, *Phys. Chem. Chem. Phys.* 2008, **10**, 6615-6620.
51 F. Weigend and R. Ahlrichs, *Phys. Chem. Chem. Phys.* 2005, **7**, 3297-3305.
52 F. Weigend, *Phys. Chem. Chem. Phys.* 2006, **8**, 1057-1065.
53 J. M. Pérez-Jorda and A. D. Becke, *Chem. Phys. Lett.* 1995, **233**, 134-137.
54 S. Kristyhn and P. Pulay, *Chem. Phys. Lett*. 1994, **229**, 175-180.
55 S. Grimme, *J. Comput. Chem*. 2006, **27**, 1787-1799.
56 S. Grimme, *Wiley Interdiscip. Rev. Comput. Mol. Sci*. 2011, **1**, 211-228.

Four halogen bonded organizations of a 1,2,2-triiodo-alkene involving geminal and/or vicinal iodine atoms were studied both by X-ray diffraction and density functional theory (DFT).

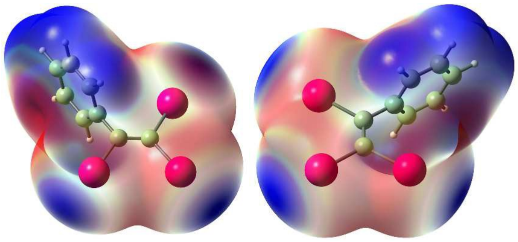

OR